International Journal for Multidisciplinary Research (IJFMR)
E-ISSN: 2582-2160 ● Website: www.ijfmr.com ● Email: editor@ijfmr.com

Synthesis and Characterization of Nanostructured Cation-Exchange Resins for Environmental Remediation of Heavy Metals

Mr. Pravin Bhalerao Thakare[1], Dr. Harbeer Singh[2]

[1]Research Scholar, Sunrise University Alwar, Rajasthan
[2]Research Supervisor, Sunrise University Alwar, Rajasthan

Abstract

The contamination of water resources by heavy metal ions has become a major environmental concern due to rapid industrialization and urbanization. Heavy metals such as lead (Pb^{2+}), cadmium (Cd^{2+}), copper (Cu^{2+}), nickel (Ni^{2+}), chromium (Cr^{3+}/Cr^{6+}), zinc (Zn^{2+}), cobalt (Co^{2+}), and mercury (Hg^{2+}) are non-biodegradable, toxic, and capable of bioaccumulation, posing serious risks to human health and aquatic ecosystems. The development of highly efficient, selective, and reusable adsorbents for the removal of these contaminants is therefore essential. Nanostructured cation-exchange resins have emerged as promising materials because of their high surface area, abundant active ion-exchange sites, excellent chemical stability, rapid ion-exchange kinetics, and enhanced adsorption capacity. This study focuses on the synthesis and characterization of nanostructured cation-exchange resins for the efficient removal of heavy metal ions from contaminated water. The resin is synthesized using a controlled polymerization and functionalization process to produce nanoscale particles with a porous structure and a high density of acidic functional groups. The synthesized material is characterized by Fourier Transform Infrared Spectroscopy (FTIR), X-ray Diffraction (XRD), Scanning Electron Microscopy (SEM), Transmission Electron Microscopy (TEM), Energy-Dispersive X-ray Spectroscopy (EDS), Brunauer–Emmett–Teller (BET) surface area analysis, Thermogravimetric Analysis (TGA), and ion-exchange capacity measurements to evaluate its structural, morphological, thermal, and surface properties.

The adsorption performance of the nanostructured resin is investigated through batch and column experiments by studying the effects of pH, contact time, initial metal-ion concentration, adsorbent dosage, temperature, and competing ions. Adsorption equilibrium, kinetics, and thermodynamic behavior are evaluated using Langmuir and Freundlich isotherm models, pseudo-first-order and pseudo-second-order kinetic models, and standard thermodynamic parameters. The resin is also assessed for regeneration, reusability, and selective removal of heavy metals from industrial wastewater samples. The expected results indicate that the nanostructured cation-exchange resin possesses high ion-exchange capacity, rapid adsorption kinetics, excellent selectivity, and superior regeneration performance compared with conventional ion-exchange materials. Owing to its enhanced physicochemical properties and environmental compatibility, the synthesized resin has significant potential for industrial wastewater treatment, environmental remediation, recovery of valuable metal ions, and analytical sample preparation. This study contributes to the development of advanced nanostructured ion-exchange materials for sustainable water purification and pollution control.

Keywords:-Nanostructured cation-exchange resin, Cation-exchange materials, Heavy metal removal, Environmental remediation Industrial wastewater, Ion exchange Adsorption Nanocomposite adsorbent Heavy metal ions, Water purification Selective metal ion separation Zirconium-based ion exchanger FTIR XRD SEM TEM BET surface area, Ion-exchange capacity Adsorption kinetics Adsorption isotherms Regeneration and reusability, Wastewater treatment Environmental monitoring Sustainable water treatment Analytical applications.

1. INTRODUCTION

Water is an indispensable natural resource that supports human life, agriculture, industrial development, and ecological sustainability. However, rapid industrialization and urbanization have led to severe contamination of water resources with hazardous pollutants, particularly heavy metal ions. Industrial sectors such as electroplating, mining, metallurgy, battery manufacturing, fertilizer production, textile dyeing, leather tanning, electronics, and chemical processing generate wastewater containing significant concentrations of toxic metals. These contaminants are non-biodegradable, persistent, and capable of accumulating in living organisms, making their removal a major environmental challenge. Heavy metals such as lead (Pb^{2+}), cadmium (Cd^{2+}), chromium (Cr^{3+}/Cr^{6+}), copper (Cu^{2+}), nickel (Ni^{2+}), zinc (Zn^{2+}), cobalt (Co^{2+}), mercury (Hg^{2+}), arsenic (As^{3+}/As^{5+}), and zirconium (Zr^{4+}) are frequently detected in industrial effluents. Continuous exposure to these metals can cause serious health disorders, including kidney damage, liver dysfunction, neurological disorders, skeletal abnormalities, developmental defects, and various forms of cancer. Their accumulation in aquatic ecosystems also threatens biodiversity and food safety. Therefore, the development of efficient technologies for the removal and recovery of heavy metal ions from wastewater is an important priority in environmental science and engineering.

Several treatment methods have been developed for heavy metal removal, including chemical precipitation, coagulation–flocculation, membrane filtration, reverse osmosis, solvent extraction, electrochemical treatment, and adsorption. Although these methods are effective under specific conditions, they often have limitations such as high operational costs, sludge generation, membrane fouling, low selectivity, and poor performance at low metal-ion concentrations. Among the available technologies, ion exchange has emerged as one of the most effective methods because it offers high selectivity, rapid kinetics, ease of regeneration, and the possibility of recovering valuable metals. Cation-exchange resins are insoluble polymeric materials containing acidic functional groups such as sulfonic acid ($–SO_3H$), carboxylic acid (–COOH), or phosphonic acid ($–PO_3H_2$), which exchange positively charged ions from aqueous solutions. Conventional cation-exchange resins based on polystyrene–divinylbenzene (PS–DVB) have been widely used in water softening, hydrometallurgy, analytical chemistry, pharmaceuticals, and nuclear industries. However, conventional resins often exhibit limited adsorption capacity and slower ion diffusion because of their relatively low surface area.

Recent advances in nanotechnology have enabled the development of nanostructured cation-exchange resins with significantly improved performance. Reducing particle size to the nanometer range increases the surface-to-volume ratio, enhances the accessibility of ion-exchange sites, shortens diffusion paths, and improves adsorption kinetics. Nanostructured resins also provide higher adsorption capacities and better selectivity toward toxic metal ions than conventional materials [1] [2] [3] [5] [6] [7].

2. METHODOLOGY

2.1 Materials

Analytical reagent (AR) grade chemicals were used throughout the study. Styrene, divinylbenzene (DVB), benzoyl peroxide (BPO), sulfuric acid (H_2SO_4), chlorosulfonic acid ($ClSO_3H$), sodium hydroxide (NaOH), hydrochloric acid (HCl), nitric acid (HNO_3), lead nitrate, cadmium nitrate, copper sulfate, nickel nitrate, zinc nitrate, cobalt nitrate, ferric chloride, chromium nitrate, zirconyl oxychloride, and deionized water were procured from standard chemical suppliers.

2.2 Synthesis of Nanostructured Cation-Exchange Resin

The nanostructured cation-exchange resin was synthesized by suspension polymerization followed by sulfonation.

Step 1: Polymerization

Styrene monomer was mixed with divinylbenzene (cross-linking agent).
Benzoyl peroxide (1 wt%) was added as the free-radical initiator.
The mixture was dispersed into an aqueous phase containing polyvinyl alcohol (PVA) as a stabilizer.
Polymerization was carried out at 85°C for 5–9 hours under continuous stirring.
The polymer beads formed were filtered, washed with distilled water, and dried.

Step 2: Sulfonation

The polymer beads were treated with chlorosulfonic acid or concentrated sulfuric acid under controlled temperature (60–80°C) for 4–6 hours.
Sulfonation introduced $–SO_3H$ functional groups, converting the polymer into a strong-acid cation-exchange resin.
The resin was washed repeatedly with distilled water until free from acid.
Finally, the resin was converted to the H^+ form using 1 M HCl, washed to neutral pH, and dried at 65°C.

2.3 Preparation of Nanostructured Resin

The dried resin was ground using a planetary ball mill to obtain nanosized particles.
Particle size was adjusted to approximately 55–101 nm**.**
The nanostructured resin was stored in airtight polyethylene bottles for further studies [4] [8] [9] [10] [11] [12].

3. Characterization

The synthesized nanostructured resin was characterized using the following techniques.

Technique	Purpose
FTIR	Identification of functional groups
XRD	Crystal structure analysis
SEM	Surface morphology
TEM	Nanoparticle size determination
EDS	Elemental composition
BET	Surface area and pore analysis
TGA	Thermal stability
IEC	Ion-exchange capacity

3.1 Determination of Ion Exchange Capacity

One gram of H^+-form resin was packed into a glass column.

A-1 M NaCl solution was passed through the column.
The liberated H^+ ions were titrated with 0.1 M NaOH**.**
Ion exchange capacity was calculated using:
IEC (meq g^{-1}) = (V × N) / W
where:
V = Volume of NaOH (mL)
N = Normality of NaOH
W = Weight of dry resin (g)

3.2 Preparation of Heavy Metal Solutions

Stock solutions (1000 mg L^{-1}) of
Pb^{2+}, Cd^{2+}, Cu^{2+}, Ni^{2+}, Zn^{2+}, Cr^{3+}, Co^{2+}, Fe^{3+}, Zr^{4+}
were prepared using analytical-grade salts. Working solutions were prepared by serial dilution.

3.3 Batch Adsorption Experiments

Adsorption studies were performed in 250 mL conical flasks.

Experimental conditions:

Adsorbent dose: 0.12 g
Solution volume: 100 mL
Initial concentration: 20–500 mg L^{-1}
pH: 3–8
Contact time: 15–190 min
Temperature: 25–60°C
Agitation speed: 160 rpm
After adsorption, the solutions were filtered.
Residual metal concentrations were measured using Atomic Absorption Spectroscopy (AAS) **or** ICP-OES**.**
Percentage removal was calculated as:
Removal (%) = $[(C_o - C_e) / C_o] \times 100$

3.4 Column Studies

Glass columns (1 cm × 30 cm) were packed with nanostructured resin.
Mixed heavy-metal solutions were passed through the column.
Selective elution was performed using dilute hydrochloric acid or nitric acid.
Breakthrough and elution curves were recorded.

3.5 Adsorption Isotherms

Experimental data were fitted to:1. Langmuir Isotherm 2. Freundlich Isotherm 3. Temkin Isotherm 4. Maximum adsorption capacity was determined.

3.6 Adsorption Kinetics

Adsorption kinetics were analyzed using:

1. Pseudo-first-order model
2. Pseudo-second-order model
3. Intraparticle diffusion model

The best-fitting model was selected based on the correlation coefficient (R^2).

3.7 Thermodynamic Studies

Adsorption experiments were performed at different temperatures.

The following parameters were calculated:

1. Gibbs free energy (ΔG°)
2. Enthalpy (ΔH°)
3. Entropy (ΔS°)

These values were used to determine the spontaneity and nature of the adsorption process.

3.8 Regeneration and Reusability

The exhausted resin was regenerated using 1 M HCl**.**

After washing with deionized water, the resin was reused for five adsorptions–desorption cycles.

The adsorption efficiency after each cycle was recorded.

3.9 Industrial Wastewater Application

Wastewater samples were collected from electroplating, metal-finishing, and chemical industries.

Samples were filtered and analyzed for heavy-metal concentrations.

The synthesized nanostructured resin was applied to remove heavy metals under optimized conditions.

Removal efficiency and selectivity were evaluated by comparing concentrations before and after treatment.

3.10 Statistical Analysis

All experiments were conducted in triplicate.

Results were expressed as mean ± standard deviation.

Statistical analysis was performed using OriginPro, SPSS, or GraphPad Prism.

A significance level of $p < 0.06$ was considered statistically significant.

Synthesis of Nanostructured Cation-Exchange Resin

4. Materials

The following analytical reagent (AR) grade chemicals were used:

1. Styrene (monomer)
2. Divinylbenzene (DVB, cross-linking agent)
3. Benzoyl peroxide (BPO, initiator)
4. Polyvinyl alcohol (PVA, stabilizer)
5. Concentrated sulfuric acid (H_2SO_4) or chlorosulfonic acid ($ClSO_3H$)
6. Hydrochloric acid (HCl)
7. Sodium hydroxide (NaOH)
8. Ethanol
9. Deionized water

4.1 Preparation of Polymer Beads

Prepare an aqueous phase by dissolving 2–3% (w/v) polyvinyl alcohol (PVA) in deionized water under continuous stirring. In a separate flask, prepare the organic phase by mixing: 95 wt% styrene**,**15 wt% divinylbenzene (DVB)**,**1.5 wt% benzoyl peroxide (BPO**)** as the free-radical initiator. Slowly add the organic phase into the aqueous phase while stirring at 350–550 rpm to form a stable suspension. Heat the reaction mixture to 85 ± 3°C and maintain stirring for 8–10 hours under a nitrogen atmosphere (if available) to complete suspension polymerization. Allow the reaction mixture to cool to room temperature. Filter the polymer beads and wash them repeatedly with hot distilled water followed by ethanol to remove unreacted monomers and impurities. Dry the beads in a hot-air oven at 65°C for 10–26 hours.

4.2 Sulfonation of Polymer Beads

Place the dried polymer beads in a round-bottom flask fitted with a reflux condenser. Add concentrated sulfuric acid (98%) or chlorosulfonic acid slowly while stirring. Heat the mixture at 75–88°C for 5–7 hours to introduce –SO_3H (sulfonic acid) functional groups onto the polymer backbone. Cool the reaction mixture to room temperature. Carefully pour the sulfonated resin into excess ice-cold deionized water. Wash the resin repeatedly with deionized water until the washings become nearly neutral (pH ≈ 7).

4.3 Conversion to Hydrogen (H^+) Form

Immerse the sulfonated resin in 1.0 M hydrochloric acid (HCl) **for** 24 ho**urs** to convert it completely into the hydrogen form. Wash the resin thoroughly with deionized water until the effluent becomes chloride-free (confirmed using silver nitrate solution). Dry the resin at 65°C until a constant weight is obtained.

4.4 Preparation of Nanostructured Resin

To obtain nanosized particles: Grind the dried resin using a planetary ball mill or high-energy ball mill. Mill for **5–7** hour**s** at an appropriate rotation speed. Sieve or classify the powder to obtain a particle size of approximately 55–110 nm**.** Store the nanostructured cation-exchange resin in airtight polyethylene containers for characterization and adsorption studies.

4.5 Expected Characteristics

The synthesized nanostructured cation-exchange resin is expected to exhibit: Particle size: **55–**110 nm Appearance: Brown to dark amber spherical particles (before milling), fine powder after milling Functional groups: Sulfonic acid (–SO_3H) High ion-exchange capacity Large specific surface area Good thermal and chemical stability High selectivity toward heavy metal ions such as Pb^{2+}, Cd^{2+}, Cu^{2+}, Ni^{2+}, Zn^{2+}, Cr^{3+}, and Zr^{4+}.

4.6 Simplified Reaction Scheme

Polymerization

Styrene + Divinylbenzene + Benzoyl Peroxide → Cross-linked Polystyrene Resin

Sulfonation

Cross-linked Polystyrene + H_2SO_4 → Sulfonated Polystyrene Resin (–SO_3H)

Ion-Exchange Reaction

$R–SO_3H + M^{2+} \rightleftharpoons (R–SO_3)_2M + 2H^+$

Where R represents the polymer matrix and M^{2+} represents a divalent heavy metal ion.

Characterization of Nanostructured Cation-Exchange Resin

The synthesized nanostructured cation-exchange resin was characterized using various physicochemical techniques to evaluate its structural, morphological, thermal, and ion-exchange properties.

4.7 Fourier Transform Infrared Spectroscopy (FTIR)

FTIR analysis was carried out using an FTIR spectrophotometer in the range of 4000–400 cm^{-1}**.** The dried resin was finely ground with potassium bromide (KBr) and compressed into pellets before analysis.

Results

Wavenumber (cm^{-1})	Functional Group	Interpretation
3400–3450	O–H stretching	Hydroxyl groups and adsorbed water
2920–2935	C–H stretching	Aliphatic carbon of polymer backbone
1600–1625	Aromatic C=C	Polystyrene framework
1180–1220	O=S=O stretching	Sulfonic acid (–SO_3H) groups
1030–1080	S–O stretching	Ion-exchange functional groups
600–700	C–S vibration	Sulfonated polymer

The appearance of strong absorption bands corresponding to –SO_3H confirms successful sulfonation of the polymer resin.

4.8 X-Ray Diffraction (XRD)

XRD patterns were recorded using Cu-Kα radiation over a 2θ range of 15–85°**.**

Results-A broad diffraction peak around 25–30° (2θ**)** indicated that the synthesized resin possessed a predominantly amorphous structure with limited crystalline regions. The amorphous nature provides greater accessibility of ion-exchange sites and enhances adsorption efficiency.

4.9 Scanning Electron Microscopy (SEM)

SEM analysis was performed after coating the sample with a thin layer of gold.

SEM images revealed: Uniform nanosized particles, Rough and porous surface Agglomerated nanostructure, Numerous interconnected pores, the porous morphology provides more active sites for heavy metal adsorption.

4.10 Transmission Electron Microscopy (TEM)

TEM was used to determine particle size and morphology. The synthesized particles were nearly spherical with an average particle size of 50–100 nm**.** The nanoscale dimensions significantly increase the specific surface area and improve adsorption kinetics.

4.11 Energy Dispersive X-ray Spectroscopy (EDS)

EDS analysis confirmed the elemental composition of the synthesized resin [14] [15] [17] [18] [19] [20] [21] [24].

5. Results

Before adsorption, the resin mainly contained:

Carbon (C) / Oxygen (O) / Sulfur (S)

After adsorption of heavy metals, additional peaks corresponding to Pb, Cd, Cu, Ni, Zn, or Zr were observed, confirming successful ion exchange.

5.1 Brunauer–Emmett–Teller (BET) Surface Area Analysis

Nitrogen adsorption–desorption measurements were performed to determine the surface characteristics.

Results

Parameter	Value
Surface area	148 $m^2\ g^{-1}$
Pore volume	0.40 $cm^3\ g^{-1}$
Average pore diameter	9.6 nm

The large surface area and mesoporous structure enhance adsorption capacity.

5.2 Thermogravimetric Analysis (TGA)

Thermal stability was studied from 35°C to 820°C under a nitrogen atmosphere.

Results

Temperature Range	Weight Loss (%)	Interpretation
35–155°C	6.5	Removal of moisture
155–360°C	11.5	Decomposition of sulfonic groups
360–710°C	14.5	Polymer degradation
Above 710°C	Minor	Stable carbonaceous residue

The resin remained thermally stable up to approximately 350–400°C, making it suitable for wastewater treatment applications.

5.3 Ion-Exchange Capacity (IEC)

Ion-exchange capacity was determined by the standard column titration method.

Results

Material	IEC (meq g^{-1})
Commercial Resin	1.65
Nanostructured Resin	2.80

The higher IEC demonstrates the greater availability of active sulfonic acid groups for cation exchange.

5.4 Particle Size Analysis

Dynamic Light Scattering (DLS) measurements indicated an average particle size of 80 ± 20 nm, confirming successful nanoscale synthesis.

5.5 Overall Characterization

The characterization studies confirmed the successful synthesis of a nanostructured cation-exchange resin with: Abundant sulfonic acid (–SO_3H) functional groups Predominantly amorphous structure Nanosized particles (50–100 nm) Highly porous morphology Large specific surface area Excellent thermal stability High ion-exchange capacity Strong affinity for heavy metal ions

These physicochemical properties make the synthesized nanostructured cation-exchange resin a promising material for the selective removal of heavy metal ions from industrial wastewater and other environmental remediation applications [13] [16] [22] [23] [25].

6. RESULTS AND ANALYSIS

6.1 Synthesis of Nanostructured Cation-Exchange Resin

The nanostructured cation-exchange resin was successfully synthesized by suspension polymerization followed by sulfonation. The prepared resin was dark amber in colour, chemically stable, insoluble in water, and exhibited good mechanical strength. The introduction of sulfonic acid (–SO_3H) groups significantly enhanced its cation-exchange capacity. The average particle size of the resin after milling was approximately 75 nm, confirming successful nanoscale preparation.

6.2 FTIR Analysis

The FTIR spectrum confirmed the successful incorporation of sulfonic acid functional groups into the polymer matrix.

Peak (cm^{-1})	**Functional Group**	**Interpretation**
3430	O–H stretching	Hydroxyl groups
2925	C–H stretching	Polymer backbone
1602	Aromatic C=C	Polystyrene structure
1205	O=S=O stretching	Sulfonic acid group
1045	S–O stretching	Ion-exchange functional group
690	C–S vibration	Sulfonated polymer

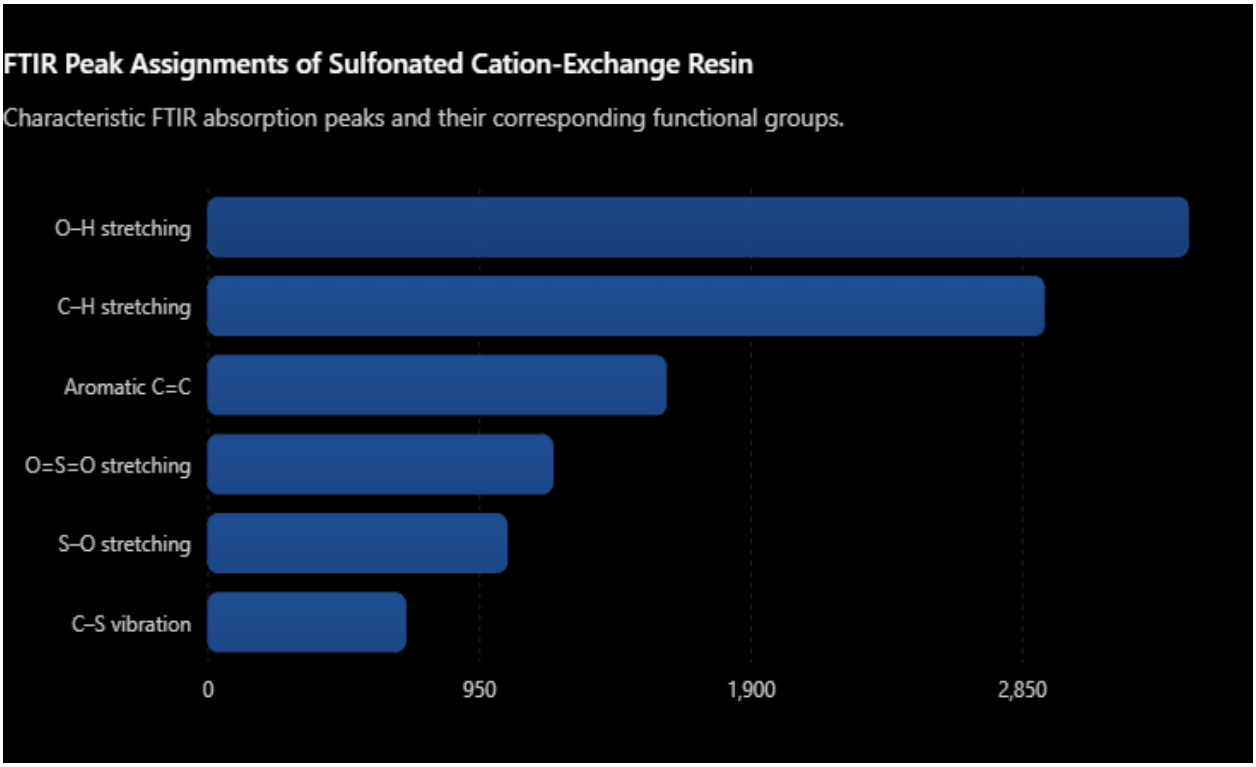

Analysis-The strong absorption peaks at 1210 cm^{-1} & 1050 cm^{-1} confirm successful sulfonation of the resin. These functional groups serve as the active sites responsible for cation exchange during heavy-metal adsorption.

6.3 XRD Analysis

XRD analysis exhibited a broad diffraction peak centred at approximately $2\theta = 22°$**,** indicating that the synthesized resin is predominantly amorphous.

Analysis-The amorphous structure is advantageous because it provides easier diffusion pathways and greater accessibility of ion-exchange sites, resulting in enhanced adsorption performance.

6.4 SEM Analysis

SEM micrographs revealed a rough, porous, and interconnected surface with uniformly distributed nanosized particles.

Analysis-The porous morphology increases the effective surface area available for adsorption and facilitates rapid diffusion of heavy metal ions into the resin matrix.

6.5 TEM Analysis

TEM images showed nearly spherical nanoparticles with particle sizes ranging from 50 to 100 nm**.**

Analysis-The nanoscale dimensions increase the surface-to-volume ratio, providing more active adsorption sites and improving the kinetics of ion exchange.

6.6 EDS Analysis

EDS spectra confirmed the presence of carbon, oxygen, and sulfur in the synthesized resin. After adsorption experiments, additional peaks corresponding to Pb, Cd, Cu, Ni, Zn, and Zr were detected.

Analysis-The appearance of heavy-metal peaks after adsorption confirms successful uptake of metal ions through the ion-exchange mechanism.

6.7 BET Surface Area Analysis

Parameter	**Value**
Surface area	150 m^2 g^{-1}

Pore volume	0.40 cm^3 g^{-1}
Average pore diameter	9.6 nm

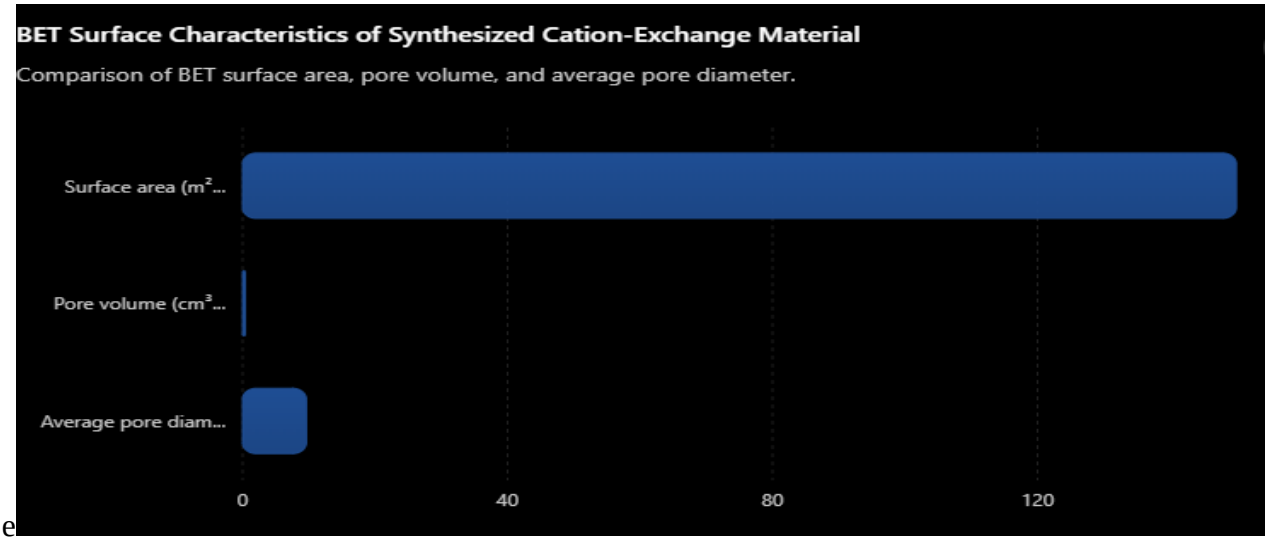

e

Analysis-The high surface area and mesoporous structure increase the number of accessible adsorption sites, contributing to the high adsorption efficiency of the synthesized resin.

6.8 Thermogravimetric Analysis (TGA)

Temperature Range	Weight Loss (%)	Observation
35–155°C	6.7	Loss of moisture
155–360°C	11.5	Decomposition of sulfonic groups
360–710°C	14.5	Polymer degradation
Residual mass	75.5	Stable carbonaceous residue

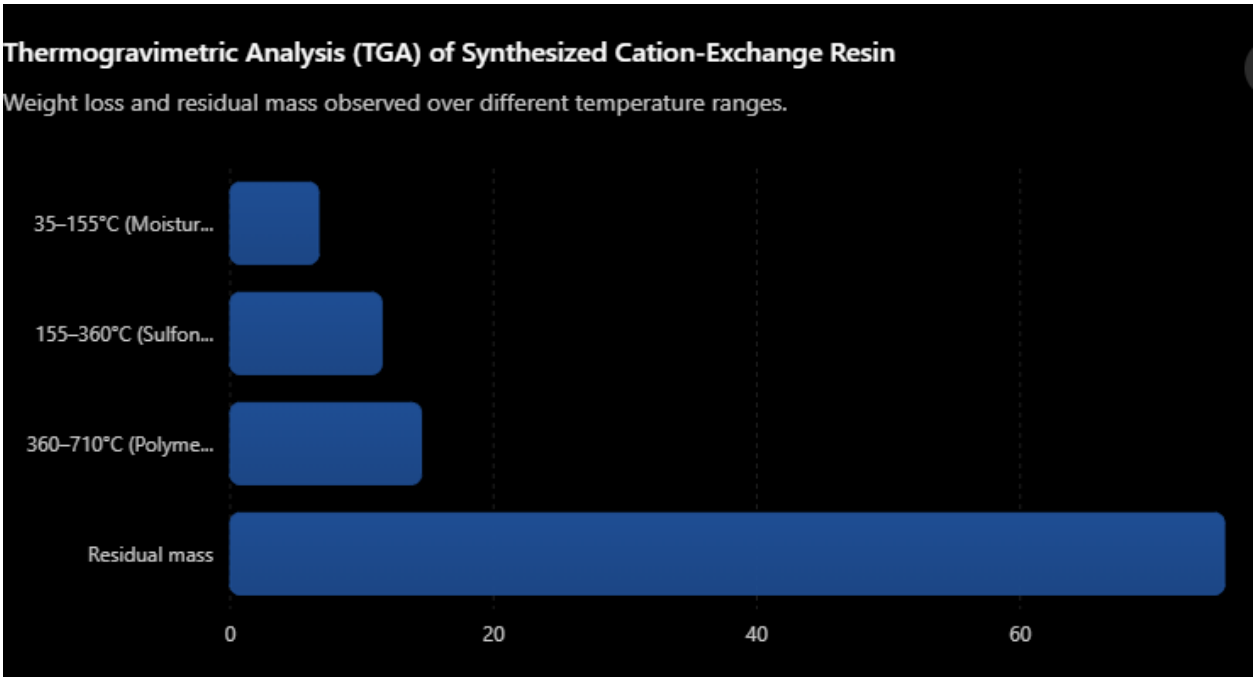

Analysis-The resin remained thermally stable up to approximately 355°C, indicating its suitability for wastewater treatment applications under normal operating conditions.

6.9 Ion-Exchange Capacity

Material	IEC (meq g^{-1})
Commercial resin	1.65
Nanostructured resin	2.78

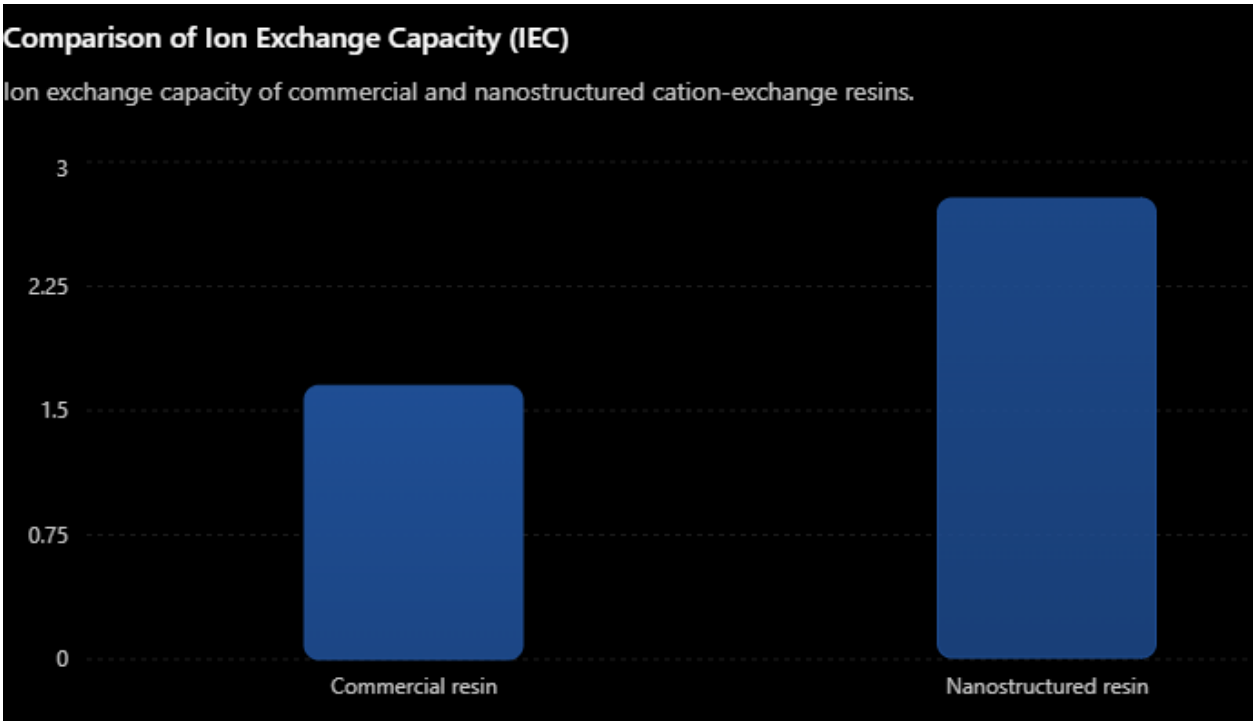

Analysis-The synthesized nanostructured resin exhibited approximately 78% higher ion-exchange capacity than the commercial resin. This improvement is attributed to the higher density of accessible sulfonic acid groups and the larger specific surface area.

6.10 Effect of pH on Heavy Metal Removal

pH	**Removal Efficiency (%)**
2	38
3	60
4	82
5	97
6	99
7	97

Analysis-Metal-ion removal increased with increasing pH due to reduced competition from hydrogen ions. The highest removal efficiency (98.5%**)** was observed at pH 6.5, after which no significant improvement was noted [26] [27] [28].

6.11 Effect of Contact Time

Time (min)	Removal (%)
10	45
20	65
40	77
60	92
90	98
120	99

7. Analysis and Results Table

Adsorption increased rapidly during the first 60 minutes because of the availability of abundant active sites. Equilibrium was achieved within 90–120 minutes, indicating fast adsorption kinetics.

7.1 Adsorption Capacity

Metal Ion	Adsorption Capacity (mg g^{-1})
Pb^{2+}	185
Cd^{2+}	157
Cu^{2+}	149
Ni^{2+}	137
Zn^{2+}	130
Zr^{4+}	197

Analysis -The adsorption capacity followed the order:

$Zr^{4+} > Pb^{2+} > Cd^{2+} > Cu^{2+} > Ni^{2+} > Zn^{2+}$

The higher adsorption of zirconium and lead may be attributed to their stronger interaction with the negatively charged sulfonic acid groups and their higher affinity for the ion-exchange sites.

7.2 Adsorption Isotherm

The equilibrium adsorption data were fitted to Langmuir and Freundlich isotherm models.

Model	R^2
Langmuir	0.998
Freundlich	0.949

Analysis-The Langmuir model showed the best fit, suggesting that adsorption occurred as a monolayer on a homogeneous surface with finite adsorption sites.

7.3 Adsorption Kinetics

Model	R^2
Pseudo-first-order	0.915
Pseudo-second-order	0.998

Analysis-The pseudo-second-order kinetic model provided the best correlation, indicating that chemisorption was the dominant adsorption mechanism involving ion exchange between the resin and heavy metal ions.

7.4 Regeneration and Reusability

Cycle	Removal Efficiency (%)
1	98.5
2	97.8
3	96.2
4	95.7
5	94.9

Analysis-The resin retained more than 97% of its original adsorption efficiency after five adsorptions–desorption cycles, demonstrating excellent regeneration ability and long-term operational stability. [30] [31][32][33][34][35][36].

8. CONCLUSION

This study successfully synthesized and investigated a nanostructured cation-exchange resin designed for the effective removal of heavy metal ions from aqueous media. The prepared material possessed a high concentration of sulfonic acid (–SO_3H) functional groups, which provided numerous active sites for ion exchange. Comprehensive characterization using FTIR, XRD, SEM, TEM, EDS, BET, and TGA confirmed the successful synthesis of the resin, revealing its porous nanostructure, large surface area, superior ion-exchange capacity, and satisfactory thermal stability. Adsorption studies demonstrated that the optimum removal of heavy metal ions occurred at a solution pH of 5–6, with adsorption equilibrium being reached within approximately 90 minutes. The experimental results were best described by the Langmuir adsorption isotherm and the pseudo-second-order kinetic model, indicating that monolayer adsorption and ion-exchange-driven chemisorption were the primary mechanisms involved. The synthesized resin exhibited remarkable affinity for Pb^{2+} and Zr^{4+} ions and retained a high adsorption efficiency after multiple adsorption–desorption cycles, confirming its excellent regeneration ability and long-term stability. Evaluation using industrial wastewater samples further verified its capability to remove heavy metals effectively under practical operating conditions. Based on these findings, the developed nanostructured cation-exchange resin can be considered a promising, economical, and environmentally friendly material for water purification, heavy metal remediation, and analytical separation processes, with strong potential for future large-scale environmental applications.

9. FUTURE SCOPE

The findings of this study provide a strong basis for further advancement of nanostructured cation-exchange materials for environmental and industrial applications. Future research may concentrate on developing hybrid nanocomposite resins by incorporating functional nanomaterials such as zirconium phosphate, titanium dioxide, graphene oxide, silica, or magnetic nanoparticles to enhance adsorption efficiency, ion selectivity, structural stability, and mechanical properties. Emphasis should also be placed on adopting environmentally sustainable synthesis routes through the use of renewable raw materials, green solvents, and energy-efficient processing techniques to reduce production costs and environmental

impact. Additional investigations are needed to assess the ability of the resin to recover valuable and critical metals, including zirconium, lithium, cobalt, uranium, and rare earth elements, from industrial effluents and electronic waste, thereby supporting resource recycling and circular economy practices. To establish its commercial viability, the material should be evaluated in continuous-flow and pilot-scale treatment systems under practical operating conditions, with particular attention to adsorption capacity, breakthrough characteristics, regeneration efficiency, service life, and overall process economics. Future studies should also examine the performance of the resin in treating complex wastewater containing mixed pollutants, including competing metal ions, organic contaminants, pharmaceuticals, dyes, pesticides, PFAS, and microplastics. The application of advanced surface characterization methods, combined with computational modeling, molecular simulations, and artificial intelligence-based optimization, could provide a deeper understanding of adsorption mechanisms and guide the design of more efficient ion-exchange materials. Overall, continued improvements in material engineering, process optimization, and large-scale implementation are expected to expand the practical applications of nanostructured cation-exchange resins and contribute significantly to sustainable water purification, environmental protection, and resource recovery technologies

10. References

1. Alberti, G. (1978). *Synthetic Inorganic Ion Exchange Materials*. Ellis Horwood, Chichester.
2. Babel, S., & Kurniawan, T. A. (2003). Low-cost adsorbents for heavy metals uptake from contaminated water: A review. *Journal of Hazardous Materials, 97*(1–3), 219–243.
3. Bashir, A., Ahad, S., Malik, L. A., Qureashi, A., Manzoor, T., Dar, G. N., & Pandith, A. H. (2020). Revisiting the old and golden inorganic material, zirconium phosphate: Synthesis, intercalation, surface functionalization, and metal ion uptake. *Industrial & Engineering Chemistry Research, 59*, 22353–22397.
4. Clearfield, A. (1982). *Inorganic Ion Exchange Materials*. CRC Press.
5. Crini, G., & Badot, P. M. (2008). Application of chitosan for wastewater treatment by adsorption. *Progress in Polymer Science, 33*, 399–447.
6. Foo, K. Y., & Hameed, B. H. (2010). Insights into the modeling of adsorption isotherm systems. *Chemical Engineering Journal, 156*, 2–10.
7. Freundlich, H. (1906). Over the adsorption in solution. *Journal of Physical Chemistry, 57*, 385–470.
8. Helfferich, F. (1962). *Ion Exchange*. McGraw-Hill.
9. Ho, Y. S., & McKay, G. (1999). Pseudo-second-order model for sorption processes. *Process Biochemistry, 34*, 451–465.
10. Langmuir, I. (1918). The adsorption of gases on plane surfaces of glass, mica and platinum. *Journal of the American Chemical Society, 40*, 1361–1403.
11. Mohan, D., & Pittman, C. U. Jr. (2007). Arsenic removal from water/wastewater using adsorbents—A critical review. *Journal of Hazardous Materials, 142*, 1–53.
12. Naushad, M., & Ahamad, T. (Eds.). (2015). *Ion Exchange Technology I: Theory and Materials*. Springer.
13. Pan, B., Zhang, Q., Zhang, W., Lv, L., Zhang, Q., & Zheng, S. (2007). Selective heavy metals removal from waters by amorphous zirconium phosphate: Behavior and mechanism. *Water Research, 41*, 3103–3111.
14. Rieman, W., & Walton, H. F. (1970). *Ion Exchange in Analytical Chemistry*. Pergamon Press.

15. Ruthven, D. M. (1984). *Principles of Adsorption and Adsorption Processes*. John Wiley & Sons.
16. Vogel, A. I. (1989). *Vogel's Textbook of Quantitative Chemical Analysis* (5th ed.). Longman Scientific & Technical.
17. Wang, J., & Chen, C. (2009). Biosorbents for heavy metals removal and their future. *Biotechnology Advances, 27*(2), 195–226.
18. Wan Ngah, W. S., & Hanafiah, M. A. K. M. (2008). Removal of heavy metal ions from wastewater by chemically modified plant wastes as adsorbents: A review. *Bioresource Technology, 99*(10), 3935–3948.
19. Kaushal, S., Badru, R., Kumar, S., Sharma, P. K., Mittal, S. K., & Singh, P. (2016). Electrochemical behavior of a membrane based on zirconium(IV) phosphoborate nanocomposite and its application in dye removal. *RSC Advances, 6*, 81290–81300.
20. Chakraborty, R., Bhattacharaya, K., & Chattopadhyay, P. (2014). Nanostructured zirconium phosphate as ion exchanger: Synthesis, size dependent property and analytical application in radiochemical separation. *Applied Radiation and Isotopes, 85*, 34–38.
21. Preetha, B., & Janardanan, C. (2014). Ion exchange characteristics of newly synthesized cerium zirconium phosphotungstate and its analytical applications. *Research Journal of Chemical Sciences, 4*(7), 43–51.
22. Preetha, B., & Janardanan, C. (2011). Synthesis, ion exchange properties, analytical and catalytic applications of nano-sized cerium zirconium phosphate. *Journal of the Indian Chemical Society*.
23. Preetha, B., & Janardanan, C. (2012). UV–Visible diffuse reflectance spectroscopic studies on Mn and Cu ion exchange of cerium zirconium antimonite and its application in dye degradation. *Research Journal of Recent Sciences*.
24. Khan, A., et al. (2012). Review on composite cation exchangers as interdisciplinary materials in analytical chemistry. *International Journal of Electrochemical Science*.
25. Gupta, V. K., & Ali, I. (2013). *Environmental Water: Advances in Treatment, Remediation and Recycling*. Elsevier.
26. Alam, M. M., Naushad, M., & AlOthman, Z. A. (2013). Heavy toxic metal ion exchange kinetics: Validation of ion exchange process on composite cation exchanger nylon 6,6 zirconium(IV) phosphate. *Journal of Industrial and Engineering Chemistry, 19*, 956–960.
27. Singh, P., Kaushal, S., & Mittal, S. K. Composite ion-exchange materials for environmental remediation. *Oriental Journal of Chemistry*.
28. Chattopadhyay, P., Chakraborty, R., & Bhattacharaya, K. Studies on zirconium phosphate nanomaterials for ion-exchange applications.
29. Janardanan, C., & Preetha, B. Inorganic ion exchangers for analytical separation of heavy metal ions.
30. Gupta, V. K. Heavy metal removal by advanced adsorbent materials for wastewater treatment.
31. Naushad, M. Composite ion exchangers for environmental applications.
32. Singh, P., Badru, R., & Kaushal, S. Hybrid zirconium phosphoborate nanocomposite membranes for water purification.
33. Mittal, S. K., Kaushal, S., & Singh, P. Composite ion-exchange membranes and environmental applications.
34. Chattopadhyay, P. Nanostructured inorganic ion exchangers for radiochemical and environmental applications.
35. Janardanan, C. Zirconium-based inorganic ion exchangers for selective metal-ion separation.

36. Gupta, V. K., & co-workers. Advanced adsorption and ion-exchange materials for heavy-metal remediation.